Using the reversible inhibition of gastric lipase by Orlistat for investigating simultaneously lipase adsorption and substrate hydrolysis at the lipid–water interface

Anaïs Bénarouche, Vanessa Point, Frédéric Carrière, Jean-François Cavalier

Using the reversible inhibition of gastric lipase by Orlistat for investigating simultaneously lipase adsorption and substrate hydrolysis at the lipid-water interface

Anaïs Bénarouche,[†] Vanessa Point,[†] Frédéric Carrière* and Jean-François Cavalier*

CNRS - Aix-Marseille Université - Enzymologie Interfaciale et Physiologie de la Lipolyse - UMR 7282, 31 chemin Joseph Aiguier, 13402 Marseille cedex 20, France

[†] Both authors should be considered as equal first authors, and are listed in alphabetical order.

*To whom correspondence should be addressed:

Phone: +33 491164093 (JFC). Fax: +33 491715857. Emails: jfcavalier@imm.cnrs.fr; carriere@imm.cnrs.fr

Abbreviations: CMC, critical micellar concentration; DGL, dog gastric lipase; FFA, free fatty acid; HGL, human gastric lipase; HCEL, human carboxylester lipase; HPL, human pancreatic lipase ; MAG, monoacylglycerol ; TAG, triacylglycerol.

Abstract

The lipolysis reaction carried out by lipases at the water-lipid interface is a complex process including enzyme conformational changes, adsorption/desorption equilibrium and substrate hydrolysis. Mixed monomolecular films of the lipase inhibitor Orlistat and 1,2-dicaprin were used here to investigate the adsorption of dog gastric lipase (DGL) followed by the hydrolysis of 1,2-dicaprin. The combined study of these two essential catalysis steps was made possible thanks to the highest affinity of DGL for Orlistat than 1,2-dicaprin and the fact that the inhibition of DGL by Orlistat is reversible. Upon DGL binding to mixed 1,2-dicaprin/Orlistat monolayers, an increase in surface pressure reflecting lipase adsorption was first recorded. Limited amounts of Orlistat allowed to maintain DGL inactive on 1,2-dicaprin during a period of time that was sufficient to determine DGL adsorption and desorption rate constants. A decrease in surface pressure reflecting 1,2-dicaprin hydrolysis and product desorption was observed after the slow hydrolysis of the covalent DGL-Orlistat complex was complete. The rate of 1,2-dicaprin hydrolysis was recorded using the surface barostat technique. Based on a kinetic model describing the inhibition by Orlistat and the activity of DGL on a mixed 1,2-dicaprin/Orlistat monolayer spread at the air-water interface combined with surface pressure measurements, it was possible to monitor DGL adsorption at the lipid-water interface and substrate hydrolysis in the course of a single experiment. This allowed to assess the k_{cat}/K^*_M ratio for DGL acting on 1,2-dicaprin monolayer, after showing that mixed monolayers containing a low fraction of Orlistat were similar to pure 1,2-dicaprin monolayers.

Keywords: enzyme kinetics, interfacial enzymology, lipase, lipolysis, monomolecular film, lipase inhibition

1. Introduction

Inhibiting digestive lipases to reduce fat absorption has become the main pharmacological approach for the treatment of obesity during the last decade [1, 2]. The FDA-approved lipase inhibitor Orlistat is currently found in two different drug products, Xenical™ (Roche) which can be obtained only under medical prescription, and Alli™ (GlaxoSmithKline) which is an over-the-counter product. Orlistat is an active site-directed inhibitor that forms a stoichiometric long-lived acyl-enzyme complex with human gastric (HGL) and pancreatic (HPL) lipases [3-5] after the nucleophilic attack of the catalytic serine residue on the β-lactone group [6, 7] (Scheme 1). By covalently blocking the digestive lipase's active site, Orlistat inhibits the hydrolysis of dietary triacylglycerols (TAGs) and thus reduces the production and subsequent intestinal absorption of monoacylglycerols (MAGs) and free fatty acids (FFAs). The inhibitory efficacy of Orlistat is tightly associated with its amphiphilic structure. It can be found at the lipid-water interface as well as in mixed micelles with surfactants. The inhibition of HPL [7], HGL [5] and human carboxyl ester lipase (HCEL) [3] by Orlistat is thus drastically increased upon adding bile salts above their critical micellar concentration (CMC). Tiss et al. [8, 9] reported that the dependence of HPL inhibition on the presence of bile salts in the incubation medium may be attributable to the formation of mixed micelles of Orlistat and bile salts. This micellar solubilisation probably increases the availability of this inhibitor in solution and thus favours its interaction with pancreatic lipase, which active site becomes accessible in solution in the presence of bile salts [10]. Orlistat is also soluble in oil and can partition between the oil core and the lipid-water interface. Increasing the interfacial area by an emulsification process promotes a stronger diffusion of Orlistat from the oil core towards the interface [11, 12]. Taking into account these findings, it was concluded that the partitioning of Orlistat between the oil and aqueous phases, as well as its rate of transfer, may contribute importantly to the inhibition of lipolysis along the gastrointestinal tract [11].

Another factor that may be of importance is the reversibility of lipase inhibition by Orlistat (Scheme 1B). Although it is often written in literature reviews that Orlistat is an irreversible lipase inhibitor, it was shown in early studies that HCEL inhibition was reversible [3]. The authors reported that the stoichiometric acyl-enzyme complex **1** formed between the *β*-lactone ring of Orlistat and the active site serine residue of HCEL was spontaneously slowly hydrolyzed [3, 13]. Full recovery of HCEL activity was then measured concomitantly with the release of the corresponding *β*-lactone-cleavage Orlistat form (*i.e.*, compound **2** in Scheme 1). Compound **2** would also be subjected to further chemical modifications (rapid isomerization, *i.e.* compound **3**; and/or hydrolysis, *i.e.* compound **4**) leading to the *δ*-lactone final degradation product **6** together with traces of the *N*-formylleucyl ester thereof, *i.e.* corresponding to **5** [3, 13, 14]. Moreover, it was also demonstrated by the authors that these degradation products had no inhibitory activity toward lipases [14], therefore emphasizing the unique structure-inhibitory activity relationship of the Orlistat molecule. More recently, a similar reactivation phenomenon was also observed with pancreatic lipase [8]. Tiss et al. reported that the HPL inhibition by Orlistat could be rapidly and partially reversed (by around 40%) in the presence of an emulsion of short- or long-chain TAGs and bile salts below their CMC [8]. Lipolysis and lipase inhibition are thus two competitive processes that can occur simultaneously *in vitro*, as well as *in vivo* [1], when the lipase is in presence of both substrate and inhibitor. The net efficacy of the inhibitor depends on the relative rates of lipolysis and inhibition reactions, on the possible reactivation of inhibited enzyme, as well as on the relative proportions of lipid substrate and inhibitor. It was also shown that the nature and the emulsification state of dietary lipids had a large impact on these rates and on the resulting efficacy of Orlistat in the course of test meals hydrolysis [1].

In the present work, initially dedicated to dog gastric lipase (DGL) inhibition by Orlistat, a reversibility of DGL inhibition was also observed using the monomolecular film technique. More interestingly, conditions were found for observing both lipase adsorption onto the lipid film spread at the air-water interface, reactivation of Orlistat-inhibited DGL and hydrolysis of

the 1,2-dicaprin film. These unexpected findings allowed us to monitor simultaneously two essential steps of interfacial catalysis by a lipase using Orlistat as a tool. Contrary to “classical” enzymes acting on soluble substrates and often following the Michaelis-Menten model, lipases are soluble enzymes acting on an insoluble substrate, TAGs that form oil-in-water emulsions, membrane bilayers, micelles and vesicles [15-17]. In this context, lipases first need to bind the lipid-water interface before hydrolyzing their substrates. This mechanism of action often includes conformational changes at the enzyme level, such as the opening of a lid controlling the access to the active site and generating an interfacial recognition site [15, 18, 19]. It is usually rather difficult to analyze the various reaction steps of interfacial catalysis in a single experiment, and lipase assays often give access to global and apparent kinetic parameters resulting from all these steps. Since measuring the enzyme partitioning between the aqueous phase and the substrate interface is a difficult task in the course of the lipolysis reaction, lipase assays are often performed in presence of a large excess of substrate interfacial area assuming that all enzyme is bound at the interface. Lipases can however act according to a hopping mode and a continuous exchange between the water phase and the interface can occur with a specific equilibrium constant [20]. With lipid monolayers as substrate, it was shown that only part of the enzyme binds to the lipid film spread at the air-water interface using either a radio-labelled lipase (continuous assay) [21, 22] or an ELISA for detecting the lipase in the bulk phase and lipid film after their separation (end-point assay) [18, 23-25].

Using DGL as a model enzyme, the new experimental model described here aims at monitoring both lipase adsorption and activity using mixed monomolecular films of 1,2-dicaprin and Orlistat with the surface barostat technique. DGL can be used as a model lipase because gastric lipase is the first enzyme involved in fat digestion in the stomach, and like pancreatic lipase it shows a strong preference for TAGs and diacylglycerols (DAGs); while some other lipases prefer substrates forming aggregates in solution like MAGs [26]. Moreover, DGL has

85.7% amino acid sequence identity with HGL and both enzymes have superimposable 3-D structures [27] and similar lipase activities [28].

2. Materials and methods

2.1. Chemicals.

1,2-didecanoyl-*sn*-glycerol (1,2-dicaprin, reference 800810P) from Avanti Polar Lipids Inc. was purchased from Coger (Paris, France) and was > 99% purity. All other chemicals, including Orlistat, 2-(*N*-morpholino)ethane sulfonic acid (MES), NaCl, $CaCl_2$ and sodium acetate were purchased from Sigma-Fluka-Aldrich (St-Quentin-Fallavier, France) and were > 98% purity. Chloroform (anhydrous for analysis, stabilized with amylene) was purchased from Sigma-Aldrich-Fluka (St-Quentin-Fallavier, France) and was of HPLC grade.

2.2. Enzymes.

Crude recombinant dog gastric lipase (DGL) was provided by Meristem Therapeutics (Clermont-Ferrand, France) [29] and purified as previously described [27]. For protein digestion before mass spectrometry analysis, trypsin of sequencing grade was purchased from Sigma-Aldrich-Fluka (St-Quentin-Fallavier, France).

2.3. Protein digestion and MALDI-TOF mass spectrometry analysis.

Protein in-gel digestion was performed with sequencing grade trypsin as previously described [30]. MALDI-TOF analyses were performed on a Bruker Microflex II mass spectrometer (Daltonik, Deutchland) using a saturated solution of α-cyano-4-hydroxycinnamic acid in acidified water (0.1% TFA) and acetonitrile (30:70, v/v) as matrix. Mass spectra were acquired in the positive ion mode, using the FlexAnalysis™ software program (Bruker, Daltonik, Deutchland). Theoretical and experimental monoisotopic peptide masses were obtained using the BioTools™ software program (Bruker, Daltonik, Deutchland) with a mass tolerance ranging from 50 to 100 ppm.

2.4. Kinetics of DGL adsorption and activity using the monomolecular film technique.

Measurements were performed at room temperature (25 °C) using the KSV5000 barostat equipment (KSV, Helsinki, Finland) monitored by the KSV Device Server Software v.1.20 (KSV Instruments Ltd., Helsinki, Finland) running under Windows XP®. The principle of this method has been described previously by Verger et al. [31]. It involves the use of a Teflon "zero-order" trough with two compartments: a reaction compartment (volume 38.5 mL; surface area, 31.2 cm^2) and a reservoir compartment (volume 126.3 mL; surface area, 210.5 cm^2) connected to each other by a small surface channel. Before each experiment, the Teflon trough was cleaned with tap water, and then gently brushed in the presence of distilled ethanol, before being washed again with tap water and abundantly rinsed with Milli-Q™ water. The Teflon trough was filled with 10 mM sodium acetate buffer (pH 5.0) containing 100 mM NaCl and 20 mM $CaCl_2$, prepared with Milli-Q™ water and filtered through a 0.45 µm Millipore® membrane. Residual surface-active impurities were removed before each experiment by simultaneous sweeping and suction of the surface [21]. The monolayer was formed at the air-water interface by spreading a few microliters of a lipid solution (1 mg mL^{-1} in chloroform) until the desired initial surface pressure (Π_i), measured with a Wilhelmy plate (perimeter 3.924 cm) [32], was reached. The waiting time for the spreading solvent evaporation and for the film to reach equilibrium varied from 10 to 20 min depending on the spreading volume and the initial surface pressure.

When using mixed monomolecular films of 1,2-dicaprin containing various mole fraction of Orlistat ($\alpha_{Orlistat}$, %), a Teflon barrier was placed transversally over the small channel connecting the two compartments of the "zero-order" trough in order to block surface communication between these compartments. Surface pressure was first determined by placing the Wilhelmy plate in the reaction compartment where the mixed film was spread at the desired Π_i. The stability of each mixed 1,2-dicaprin/Orlistat monolayer was initially checked by recording over 90 min the variations in surface pressure. In all cases, no significant change in surface pressure ($\pm$ 0.2 mN m^{-1}) was observed during the time course of the experiment. The

Wilhelmy plate was then switched to the reservoir compartment where only 1,2-dicaprin film was subsequently spread at the same Π_i. The barrier between the two compartments was then removed in order to allow communication of the two films, and the enzyme solution (1.1 mg mL^{-1} DGL in 10 mM MES pH 6.0 containing 150 mM NaCl) was injected with an Hamilton syringe (from 6-50 µL for final concentrations ranging from 5-60 nM, respectively) into the subphase of the reaction compartment. With medium chain lipids such as 1,2-dicaprin, soluble lipolysis products (*i.e.*, monocaprin and capric acid) are released upon the action of the lipase and a drop in surface pressure is recorded. Using the barostat mode of the KSV5000 device, an automatically-driven Teflon mobile barrier moves over the reservoir compartment to compress the monomolecular lipid film and compensate for the substrate molecules removed from the film by the enzyme hydrolysis, thus keeping the surface pressure (*i.e.* Π_i continuously measured on the reservoir compartment) constant. With the surface barostat technique, the lipid substrate packing in the monomolecular film (*i.e*. the molecular area and surface concentration of substrate) is thus assumed to remain constant during the time-course of hydrolysis, and it is then possible to obtain accurate steady-state kinetic measurements with minimal perturbation caused by increasing amounts of reaction products. The reaction compartment was stirred with a 1-cm magnetic bar rotating at 250 rpm. The system is designed so that the agitation of the aqueous phase with a magnetic stirring bar does not disturb the stability of the surface film. The data recorded from inhibition kinetics were analyzed according to a model previously established for lipase inhibition [18]. DGL activity (mole cm^{-2} min^{-1} M^{-1}) was expressed as the number of moles of substrate hydrolyzed per time unit (min), per surface unit (cm^2) of the reaction compartment of the "zero-order" trough and for an arbitrary lipase concentration of 1 M.

2.5. Treatment of kinetics data of substrate hydrolysis by DGL at the lipid-water interface using the monomolecular film technique [31].

Under steady state conditions (*i.e.*, when time tends to infinity, Figure 2A) the maximal reaction rate $v_S = dy/dt$ (cm s^{-1}) is calculated from the slope of the experimental kinetic curves $y = f(t)$; where y is the movement of the mobile barrier (cm) monitored by the barostat and t, time (min). The enzyme velocity v_m (molecule cm^{-2} s^{-1}) in the monolayer system can be deduced from Eq. 1 [33]:

$$v_m = \Gamma_s \frac{v_s \cdot l}{S} \qquad \text{Eq. 1}$$

where Γ_S is the surface concentration of 1,2-dicaprin (molecule cm^{-2}) at Π_i = 25 mN m^{-1}, derived from the equilibrium surface pressure-area isotherm; S is the surface area of the reaction compartment (cm^2); and l is the width (cm) of the reservoir compartment. It is assumed here that the molecular area of substrate is constant and remains the same as in initial conditions, thus neglecting changes due to enzyme penetration and Orlistat degradation products before the steady state velocity regime is reached. Using the nomenclature of the Verger-de Haas interfacial kinetic model [33, 34], the expression of v_m in the monolayer system can be rewritten as (Eq. 2):

$$v_m = \frac{k_{cat}}{K_M^*} \cdot \Gamma_{E^*} \Gamma_S \qquad \text{Eq. 2}$$

where k_{cat} is the interfacial catalytic rate constant (s^{-1}); K^*_M is the interfacial Michaëlis-Menten constant (molecule cm^{-2}); and Γ_{E^*} is the interfacial concentration (molecule cm^{-2}) of the DGL adsorbed onto the film. When acting on mixed 1,2-dicaprin/Orlistat monomolecular films, the residual lipase activity ($RA_{E^*(\%)}$, %) is then deduced from Eq. 2 as the ratio of the respective enzyme velocities in presence ($v_{m(\alpha_{Orlistat})}$) and in absence ($v_{m(\alpha_{Orlistat}=0)}$) of inhibitor (Eq. 3):

$$RA_{E^*(\%)} = 100 \cdot \frac{v_{m(\alpha_{Orlistat})}}{v_{m(\alpha_{Orlistat}=0)}} \qquad \text{Eq. 3}$$

2.6. DGL adsorption/penetration onto mixed 1,2-dicaprin/Orlistat monomolecular films.

Mixed monomolecular films of 1,2-dicaprin/Orlistat were formed only over the reaction compartment of the "zero-order" Teflon trough (volume 38.5 mL; surface area, 31.2 cm^2) at an initial surface pressure (Π_i) of 25 mN m^{-1} as described above. After injecting DGL into the aqueous subphase with an Hamilton syringe (from 6.8 to 50 µL DGL stock solution for final concentrations ranging from 8.4 to 60 nM, respectively), the surface pressure increase due to the adsorption/penetration of the lipase into the mixed monolayer was continuously recorded (every 5 seconds) until the equilibrium surface pressure was reached. The aqueous subphase, composed of the same acetate buffer (pH 5.0) as described above, was continuously stirred with a 1-cm magnetic bar rotating at 250 rpm.

2.7. Treatment of kinetic data of DGL adsorption onto mixed 1,2-dicaprin/Orlistat monolayers.

The apparent kinetic parameters of DGL adsorption (k_a, M^{-1} s^{-1}) and desorption (k_d, s^{-1}) onto the mixed 1,2-dicaprin/Orlistat films were calculated according to the methodology we recently reported [35]. Briefly, the experimental data (*i.e.*, surface pressure increase ($\Delta\Pi$) with time) were fitted to the Langmuir adsorption isotherm equation adapted to surface pressure measurements (Eq. 4):

$$\Pi\,(t) = \Pi_i + \Delta\Pi_{max}.\theta.[1 - \exp\,(-\sigma.t)] \qquad \text{Eq. 4}$$

where $\Pi\,(t)$ is the surface pressure measured as a function of time; Π_i is the initial surface pressure; $\Delta\Pi_{max}$ is the maximum variation of surface pressure reached upon DGL binding; θ is the fraction of the total free adsorption (binding) sites coverage; and $\sigma = (k_a.C_{E0} + k_d)$ with C_{E0} (mol L^{-1}) being the DGL concentration in the subphase of the trough.

Curve-fitting the experimental data points to Eq. 4 using KaleidaGraph 4.1 software (Synergy Software) allowed calculating σ values for multiple C_{E0} concentrations at each Π_i investigated. Values of k_a and k_d were then determined from the slope and y-intercept, respectively, of the

linear plot of σ *versus* C_{E0} (Figure S2 in Supplementary Material). The adsorption equilibrium coefficient, K_{Ads}, which represents the binding affinity between the protein and the lipid film, was obtained from the ratio of the measured rate constants ($K_{Ads} = k_a/k_d = 1/K_D$).

Using the mathematical equations derived from the interfacial kinetic model of Verger et al. [31, 34, 36, 37], it became possible to estimate, by indirect calculation, the theoretical value of the enzyme interfacial concentration (Γ_{E*}, molecule cm^{-2}) based on Eq. 5, where S_{trough} / V_{trough} represents the surface area-volume ratio (cm^{-1}) of the reaction compartment of the Teflon trough:

$$\Gamma_{E*} = C_{E0} \Big/ \left[(1 + K_D) \cdot \left(\frac{S_{trough}}{V_{trough}} \right) \right] \qquad \text{Eq. 5}$$

Finally, the mathematical expression of the molecular area (A_{E*}, $Å^2$ $molecule^{-1}$) occupied by the enzyme adsorbed onto the mixed films at a surface pressure of 25 mN m^{-1} maintained constant by the mobile barrier movement, is:

$$A_{E*} = \left[\left(S_{trough} - A_{lipid} \cdot n_{lipid} \right) \cdot \theta \right] / \left(\Gamma_{E*} \cdot S_{trough} \right) = \left(\text{surface occupancy} \right) / \Gamma_{E*} \qquad \text{Eq. 6}$$

A_{lipid} ($Å^2$ $molecule^{-1}$) is the mean molecular area of the mixed film at a given $\alpha_{Orlistat}$ value deduced from the surface pressure (Π)-molecular area isotherms at Π_i = 25 mN m^{-1}; n_{lipid} is the number of molecules spread at the air-water interface at the same Π_i; and θ is the fractional surface coverage determined in Eq. 4.

Eq. 6, thus obtained by means of our mathematical approach based on Verger's kinetic model, therefore allowed access to an estimation of the values of A_{E*} (see reference [35] for more details).

3. Results and Discussion

3.1. Covalent inhibition of DGL by Orlistat.

It was first check that DGL was inhibited by Orlistat through a covalent interaction with the catalytic serine residue as previously demonstrated with HCEL and HPL [3, 8, 14]. After pre-incubation of DGL with a 40-fold molar excess of Orlistat for 30 min, a tryptic digestion of the inhibited DGL and a peptide mass fingerprint (PMF) by MALDI-TOF mass spectrometry [38] were performed under previously described conditions [30]. PMF was then compared with the one of the non-inhibited lipase (Figure S1 in Supplementary Material). With DGL alone, a *m/z* of 2,904.9 Da corresponding to the T^{142}GQDKLHYVGH**S**^{153}QGTTIGFIAFSTNPK^{168} peptide containing the catalytic Ser^{153} residue was detected (Figure S1A). When DGL was incubated with Orlistat, a mass increase of +500.7 Da was observed in the PMF spectrum for the peptide containing the active site serine (Figure S1B), which confirmed that a covalent bond had been formed between Orlistat (495.39 Da) and the catalytic serine residue of the gastric lipase, taking into account the precision of the MALDI-TOF technique and the molecular mass of DGL (48,449 ± 103 Da) recorded using the same instrument.

3.2. Enzyme kinetics of DGL on mixed 1,2-dicaprin films containing Orlistat.

In order to get more insight into the mechanism of inhibition of DGL in presence of Orlistat, the monolayer technique [31] and surface pressure measurements were further used to monitor the interfacial interactions between DGL and monomolecular films of 1,2-dicaprin spread at the air-water interface and containing various mole fractions ($\alpha_{Orlistat}$, %) of Orlistat. As a prerequisite to study DGL inhibition at the lipid-water interface, compression isotherms of various mixed 1,2-dicaprin/Orlistat monolayers were first performed in order to determine their interfacial properties (Figure 1A). The surface pressure (Π)-molecular area curves deduced from compression isotherms were comparable to those previously published [11]. For pure compounds, the mean value of the characteristic parameters (surface pressure, Π_{coll}; molecular

area, A_{coll}) obtained at the collapse point were: Π_{coll} = 44.9 mN m^{-1} / A_{coll} = 40.6 $Å^2$ $molecule^{-1}$ for 1,2-dicaprin (Figure 1A, isotherm 1); and Π_{coll} = 28.8 mN m^{-1} / A_{coll} = 62.1 $Å^2$ $molecule^{-1}$ for Orlistat (Figure 1A, isotherm 8). A working surface pressure of Π_i = 25 mN m^{-1} was selected from these isotherms because it is below the collapse pressure of all films and DGL was found to be active on pure 1,2-dicaprin with linear kinetics at this surface pressure (Figure 2A).

The mean molecular area of mixed monomolecular films of 1,2-dicaprin/Orlistat was further determined for various Orlistat mole fractions at this selected surface pressure of 25 mN m^{-1}. Only slight deviations from ideal mixing (straight dashed line joining the molecular areas of the pure compounds) were observed. Orlistat induced either low expansion effects at $\alpha_{Orlistat}$ above 10% (Figure 1B), or on the contrary low condensing effects at $\alpha_{Orlistat}$ below 2.0% (Figure 1C). Such variations amounted to only +7.3% at $\alpha_{Orlistat}$ = 25% and +8.2% at $\alpha_{Orlistat}$ = 0.3%. For $\alpha_{Orlistat}$ ranging from 0 to 1.5%, the mean molecular area (50.0 ±1.6 $Å^2$ $molecule^{-1}$) remained close to that of pure 1,2-dicaprin (52.2 $Å^2$ $molecule^{-1}$) at 25 mN m^{-1}.

After the characterization of mixed 1,2-dicaprin/Orlistat monolayers, DGL interaction with these monolayers and lipolytic activity was then investigated using the surface barostat technique. As shown in Figure 2A, the forward movement of the mobile barrier (*i.e.* consumption of 1,2-dicaprin substrate and rapid desorption of lipolysis products) increased progressively with time to reach a steady-state regime after a lag period (τ_1) increasing with $\alpha_{Orlistat}$. τ_1 value was defined as the intercept with time axis of the asymptote reached under steady state conditions (Figure 2A). In the absence of Orlistat, the mobile barrier moved forward after a τ_1 lag time of around 3.5 min following enzyme injection below the monolayer (Figure 2A, curve 1). When Orlistat was mixed with 1,2-dicaprin, τ_1 value increased and ranged from 18 to 80 min while increasing $\alpha_{Orlistat}$ (Table 1). Moreover, the forward movement of the mobile barrier was preceded by a transient backward movement ($\Delta L_{barrier}$, mm - Figure 2A) that could reflect an increase in the occupation of the surface of the reaction compartment by either the

enzyme adsorbed onto the monolayer or some reaction products before their desorption. This increase in the surface area was quantified as $\Delta S = \Delta L_{barrier} \times l$, l (=61 mm) being the width of the reservoir trough. Like τ_1 values, ΔS was also found to increase with $\alpha_{Orlistat}$ (Table 1).

After making these observations, τ_1 and ΔS values, as well as the enzyme velocity at steady-state regime (v_m), were further used for describing DGL interaction with the mixed monolayers, its inhibition by Orlistat, and its activity on 1,2-dicaprin. Using Eq. 3, DGL residual activity on 1,2-dicaprin ($RA_{E^*(\%)}$) was deduced from the experimental calculated v_m (Eq. 1) and plotted as a function of $\alpha_{Orlistat}$. As depicted in Figure 2B, only small amounts of Orlistat were required to significantly inhibit the DGL activity. The mole fraction of Orlistat which reduced the enzyme activity to 50% of its initial value ($\alpha_{50Orlistat}$) was found to be around 1.4%. Similar findings were obtained in previous studies [18, 39, 40], with for instance an $\alpha_{50Orlistat}$ of 0.25% in the case of HGL [39] acting on mixed 1,2-dicaprin/Orlistat monolayers spread at 20 mN m^{-1}. These results reflect a high affinity of gastric lipase for Orlistat present within a substrate monolayer. Tiss et al. have proposed that the hydrophilic parts of Orlistat, *i.e.* the reactive *β*-lactone ring and the *N*-formyl-L-Leucine group could extend more deeply in the aqueous subphase than 1,2-dicaprin molecules, because of their larger polar head groups size [11]. Such interfacial orientation might be a plausible explanation for the strong affinity of lipases for Orlistat, present in mixed film even at low mole fractions, and therefore responsible for its high inhibitory efficiency.

Interestingly for $\alpha_{Orlistat}$ values below 1.0%, experimental $RA_{E^*(\%)}$ were consistently higher than 100% (*i.e.*, $RA_{E^*(\%)}$ for $\alpha_{Orlistat}$ = 0%), with a maximum ($RA_{E^*(\%)}$ = 140%) at $\alpha_{Orlistat}$ = 0.3%. It was checked that increasing DGL concentration from 8.4 to 60.0 nM did not modify the profile of the experimental inhibition curves obtained for $\alpha_{Orlistat} \leq 1.0\%$ (Figure 2C). One hypothesis to explain this phenomenon is that the presence of Orlistat or its transient degradation products in the mixed films could trigger DGL activity at low $\alpha_{Orlistat}$ before a clear

$\alpha_{Orlistat}$–dependent inhibition profile is observed at higher $\alpha_{Orlistat}$ (Figure 2B). It was previously observed that the activity of lipolytic enzymes could be remarkably influenced by using mixed monolayers rather than pure substrate monolayers [21, 41-44]. For instance, porcine pancreatic lipase (PPL) activity on trioctanoylglycerol was doubled by progressively diluting the TAG film with non-hydrolysable dilauroylphosphatidylcholine (DLPC) [21]. DGL activity on 1,2-dicaprin could thus be increased by a more favourable presentation of the substrate to the enzyme in mixed films containing traces of Orlistat and/or its degradation products. Paradoxically, it would be the first time that this phenomenon is observed when the lipid substrate is mixed with small amounts of a lipase inhibitor. Another hypothesis could be however artefacts of calculation. Measuring an increase in residual lipase activity (more than 100% activity on 1,2-dicaprin alone) could result from an increase in substrate molecular area, higher changes in surface pressure when it is hydrolyzed and thus a larger forward movement of the mobile barrier. It is however difficult to imagine such an increase in 1,2-dicaprin molecular area at constant surface pressure, while the lipase and transient Orlistat degradation products are also present at the interface. In the present work, molecular area of 1,2-dicaprin was considered to be constant for calculations and equal to that estimated from a pure film of substrate ($A_{1,2\text{-dicaprin}}$ = 52.2 $Å^2$ $molecule^{-1}$) when all Orlistat molecules have been hydrolyzed.

Increasing the lipase concentration also resulted in a significant reduction of τ_1 lag time values up to 72-89% at 60 nM (Table 1), but did not significantly impact the observed hydrolytic step (*i.e.*, $RA_{E*\%}$ values – Figure 2C). It is noteworthy that, whatever the lipase concentration in the 8.4-60 nM range, the experimentally determined $\Delta L_{barrier}$ were found to remain nearly constant for a given $\alpha_{Orlistat}$ value. The corresponding calculated mean ΔS values were 1.30 ±0.02 cm^2, 2.28 ±0.10 cm^2 and 3.36 ±0.11 cm^2 at $\alpha_{Orlistat}$ = 0.3%, 0.5% and 1.0%, respectively. According to the interfacial kinetic model developed by Verger et al. [31, 37], τ_1 lag times as well as the increase in the surface area of the film (*i.e.* ΔS) during lipolysis, were

interpreted as being due to the rate-limiting step of enzyme adsorption ($E \leftrightarrows E^*$) onto the monolayer. In these conditions, the concomitant increase in τ_1 lag time and $\Delta L_{barrier}$ (up to ≅ -10 mm at $\alpha_{Orlistat}$ = 1.5% - Figure 2A) with $\alpha_{Orlistat}$, may be associated with DGL adsorption onto the mixed monolayer. However, since the inhibition by Orlistat has been shown to be reversible with some lipases (Scheme 1), compound **2** resulting from the hydrolysis of Orlistat (Scheme 1C) might also be responsible for the transient increase in the surface area. This more polar molecule resulting from the opening of the β-lactone ring might remain at the interface and occupied a larger molecular area. To check these hypotheses, additional experiments with a pure monomolecular film of Orlistat were performed.

3.3. Evidence for the reversibility of DGL inhibition by Orlistat.

A pure film of Orlistat was spread over both the reaction and the reservoir compartments of the zero-order trough. After DGL injection (60 nM final concentration) below the monolayer, an important backward movement of the mobile barrier was first recorded (up to -34.4 mm – Figure 2D) followed by a slow and linear forward movement of the mobile barrier. This later finding is consistent with a slow hydrolysis of Orlistat by DGL followed by the formation of soluble degradation products according to the pathway described in Scheme 1. DGL inhibition by Orlistat therefore appears as a reversible process as previously shown with HCEL and HPL [3, 8, 13]. Since Orlistat degradation leads to a forward movement of the mobile barrier, one can therefore conclude that the initial backward movement of the barrier is mainly due to enzyme adsorption and not to the accumulation at the interface of insoluble Orlistat degradation products.

From these experiments, it was possible to estimate the velocity of pure Orlistat degradation by DGL (v_m = 5.34 (±0.18) × 10^9 molecule cm^{-2} s^{-1}). This value represents around 0.40% of the lipolytic rate reached by DGL on pure 1,2-dicaprin film at the same enzyme concentration (C_{E0} = 60 nM). Making the assumption that DGL would act at the same rate on

Orlistat in mixed monolayers, all Orlistat molecules could be hydrolyzed by the lipase in 1.4 min, 2.3 min and 4.5 min at $\alpha_{Orlistat}$ of 0.3%, 0.5% and 1.0%, respectively. Although these theoretical time values are lower than the τ_1 lag times observed at the same $\alpha_{Orlistat}$ before recording DGL activity on mixed 1,2-dicaprin/Orlistat monolayers (from 4.3 to 7.2 min - Table 1), they are in the same order of magnitude. This strongly supports the hypothesis that τ_1 lag time correlates with DGL inhibition by Orlistat and subsequent reactivation, *i.e.* Orlistat consumption before the 1,2-dicaprin substrate becomes a more accessible ligand for DGL. This is the first time that the reversibility of lipase inhibition by Orlistat is observed using the monomolecular film technique and mixed films of 1,2-dicaprin and Orlistat. Previous studies of this kind conducted on other mammalian digestive lipases (*i.e.*, HGL, HPL and PPL) reported a rapid and total inactivation of the lipases without mention that the enzyme could restore some of its original activity after a long lived transient molecular poisoning induced by Orlistat[18, 39, 40]. Further studies are now required to determine whether DGL is unique among lipases or the reactivation of other lipases was previously missed using the monomolecular film technique. This second hypothesis is supported by the fact that the reversibility of HPL inhibition has been shown using the pH-stat technique [8].

3.4. Using the reversible inhibition of DGL for monitoring lipase adsorption and activity in the course of a single experiment.

At this stage of the study, it appeared that the backward and forward movements of the mobile barrier observed after injecting DGL below a mixed 1,2-dicaprin/Orlistat film were associated with lipase adsorption onto the film and substrate hydrolysis, respectively. The first step of lipase adsorption was characterized by τ_1 lag time and ΔS (the surface covered by the backward shift of the barrier). Because of the much higher affinity of DGL for Orlistat than for 1,2-dicaprin, no apparent lipase activity was recorded before the reversible inhibition of DGL by

Orlistat led to a complete conversion of Orlistat into β-hydroxyacid degradation products (Scheme 1C) that were further removed from the lipid interface. After that, a rapid hydrolysis of 1,2-dicaprin molecules by "reactivated" DGL was observed and characterized by the enzyme velocity at steady-state regime (v_m).

To confirm these assumptions, a series of independent experiments were performed under the same conditions used for hydrolysis kinetics (*i.e.*: Π_i = 25 mN m^{-1}; [DGL] = 8.4 nM; $\alpha_{Orlistat}$ = 0.3, 0.5, 1.0 or 1.5% in mixed films), except that the surface pressure was not kept constant using the barostat mode after injecting the lipase in the subphase. Variations in surface pressure were thus recorded with time as usually performed for determining adsorption kinetics on a non-hydrolysable monomolecular film [35]. In each case, an increase in the surface pressure was first observed after DGL injection, up to a plateau value that was maintained for a few minutes before a drastic drop in surface pressure occurred (Figure 3A). It was hypothesized that these typical bell-shaped variations were resulting from (*i*) the adsorption of DGL onto the mixed monolayer and (*ii*) the subsequent hydrolysis of 1,2-dicaprin and desorption of lipolysis products.

The inflexion point on the $\Delta\Pi = f(t)$ curves was then determined and the corresponding time was defined as the induction time (τ_2) for observing lipolysis product desorption and thus enzyme activity (Figure 3A). Interestingly, τ_2 values were found to be almost equal to the τ_1 values determined in previous experiments with the barostat mode, τ_1 being the lag time for measuring steady-state kinetics of 1,2-dicaprin hydrolysis (Figures 3B-C). Both τ_1 and τ_2 showed an increase that was proportional to $\alpha_{Orlistat}$ values (Figure 3C). Moreover, by varying the DGL concentration from 8.4 to 60 nM, τ_1 and τ_2 lag times not only remained almost identical but also displayed the same hyperbolic decay pattern which reached a minimum plateau value at 40 nM (Figure 3D). In the absence of Orlistat, τ_1 and τ_2 values were around 3.5 min. at C_{E0} = 8.4 nM and not experimentally observed above this concentration.

From the results obtained here after injection of DGL below mixed 1,2-dicaprin/Orlistat monolayers, it becomes obvious that the forward movement of the mobile barrier observed using the surface barostat mode (Figure 2A) and the significant drop in surface pressure observed in the absence of surface pressure control (Figure 3A) are both related to the hydrolysis of 1,2-dicaprin film by the DGL. The observation of a lag time (τ_1) or induction time (τ_2) for measuring 1,2-dicaprin hydrolysis is associated with the presence of Orlistat mixed with the substrate monolayer. Using two independent experimental set-ups for determining τ_1 and τ_2, it appeared that these characteristic time values were nearly identical and varied linearly with $\alpha_{Orlistat}$ values (Figure 2C). Both lag times are therefore characteristic of the inhibition period occurring before Orlistat is fully hydrolyzed. The lipolytic activity, recorded after $\alpha_{Orlistat}$–dependent lag times, thus reflects a complete (at low $\alpha_{Orlistat}$ values, Figure 2A) or partial (Figure 2D) reactivation of the DGL inhibited after adsorption onto the mixed lipid film. The partial reactivation of DGL after inhibition by Orlistat suggests the formation of two distinct DGL-Orlistat complexes. The first one (E^*I_o; Figure 4) being formed rapidly by covalent interaction (opening of the β-lactone ring) and later on, further hydrolyzed to restore lipase activity (fast and reversible inhibition step); while the second one (E^*I_2; Figure 4) may involve a different mode of interaction between Orlistat and DGL (probably covalent, based on mass spectrometry analysis as shown in Figure S1 in Supplementary Material) and leads to a slow and irreversible lipase inhibition (or at least a long-life lipase-inhibitor complex stable during the assay period). Such a hypothesis was previously raised by Tiss *et al.* to explain the partial reversibility of human pancreatic lipase inhibition by Orlistat in bulk assays [8].

3.5. Determination of DGL apparent interfacial kinetic parameters.

Based on the kinetic model presented in Figure 4 and assuming that the surface pressure increase recorded in presence of Orlistat was due to DGL binding to the mixed film, adsorption

kinetics at Π_i = 25 mN m^{-1} were recorded for DGL concentrations ranging from 8.4 to 60 nM and $\alpha_{Orlistat}$ values of 0.3, 0.5 and 1.0%. The adsorption (k_a) and desorption (k_d) rate constants corresponding to the interaction of DGL with the mixed film were determined by curve-fitting experimental data points (only those corresponding to an increase in surface pressure up to the inflection point) to Eq. 4 [35]. k_a and k_d values obtained for the three different $\alpha_{Orlistat}$ values (0.3%, 0.5% and 1.0%) appeared to be similar (Figure S2 in Supplementary Material) and mean values were therefore estimated: mean k_a = 7.94 (±0.21) × 10^4 M^{-1} s^{-1} and mean k_d = 6.56 (±0.42) × 10^{-4} s^{-1}.

As depicted in Figure 5A, the resulting adsorption equilibrium coefficient K_{Ads} = (k_a/k_d) remained almost constant in the 0.3-1.0% $\alpha_{Orlistat}$ range (Table S1 in Supplementary Material). From these findings and the fact that mixed 1,2-dicaprin/Orlistat monolayers show a quasi-ideal mixing for $\alpha_{Orlistat}$ values between 0.0% and 1.5% (Figure 1C), the, extrapolation of K_{Ads} value to $\alpha_{Orlistat}$ = 0 (*i.e.*, the y-intercept of the linear plot [K_{Ads} = $f(\alpha_{Orlistat})$]) was made to estimate the interfacial binding affinity ($K_{Ads\ (\alpha_{Orlistat}=0)}$ = 1.22 (±0.05) × 10^8 M^{-1}) between DGL and pure 1,2-dicaprin monolayer at a surface pressure of 25 mN m^{-1}. It is worth noticing that $K_{Ads\ (\alpha_{Orlistat}=0)}$ is nearly identical to the interfacial binding affinity determined by Chahinian et al. using DGL and a solid hydrophobic surface (K_{Ads} = 1.54 × 10^8 M^{-1}) at the same pH value of 5.0 [45], and it is in the same order of magnitude as the recently reported interfacial binding affinity between DGL and the non-hydrolysable DLPC monolayer (K_{Ads} = 0.32 × 10^8 M^{-1}) at the same pH (5.0) and the same surface pressure (Π_i = 25 mN m^{-1}) [35].

3.6. Estimation of the amount of DGL adsorbed onto mixed monolayers.

From the experimentally-determined adsorption kinetic parameters (k_a, k_d, K_{Ads}), it was then possible to estimate, by means of Eq. 5, the theoretical surface concentration of adsorbed

DGL (Γ_{E*}, molecule cm^{-2}) onto the mixed films for each of the three Orlistat mole fractions tested (Table S1 in Supplementary Material).

As previously observed with K_{Ads} (Figure 5A), Γ_{E*} values did not vary significantly as a function of $\alpha_{Orlistat}$ (Figure 5B). An extrapolation to $\alpha_{Orlistat} = 0$ was then made to estimate the apparent interfacial concentration of DGL ($\Gamma_{E*(\alpha_{Orlistat}=0)}$ = 66.1 (±0.28) × 10^{10} molecule cm^{-2}) adsorbed on a pure 1,2-dicaprin monomolecular film spread at 25 mN m^{-1} over a buffer at pH 5.0. Knowing the area of the reaction compartment and the amounts of DGL injected in the subphase, it was estimated that around 10.6% of DGL was adsorbed onto the lipid film, while 89.4% DGL would remain in the bulk phase, assuming that the adsorption of the lipase onto the Teflon surface of the trough is negligible. This was previously shown in the case of human gastric lipase (HGL) using an ELISA for estimating HGL recovery in the bulk phase and monolayer [18, 23, 24]. Using Eq. 6, the surface areas occupied by a single molecule of the adsorbed protein (A_{E*}, Å^2 molecule^{-1}) onto the latter mixed films were calculated (Table S1 in Supplementary Material), and the corresponding values were plotted as a function of the relative surface increase (mean $\Delta S/S$ - Table 1) related to $\alpha_{Orlistat}$ (Figure 5C). From both $\Delta S/S$ and A_{E*} values deduced from two independent experiments, the limiting area ($A_{E*(\alpha_{Orlistat}=0)}$ = 738 ±22 Å^2 molecule^{-1}) occupied by the first DGL molecules adsorbed onto 1,2-dicaprin film could be estimated by extrapolating A_{E*} at zero relative surface increase (*i.e.*, $\Delta S/S = 0$ corresponding to $\alpha_{Orlistat} = 0$; Figure 5C) according to the method reported by Bougis et al. [46].

It is noteworthy that these data, $\Gamma_{E*(\alpha_{Orlistat}=0)}$ and $A_{E*(\alpha_{Orlistat}=0)}$, are very close to those recently estimated ($\Gamma_{E*\text{-DLPC}}$ = 49.0 × 10^{10} molecule cm^{-2}; $A_{E*\text{-DLPC}}$ = 674 Å^2 molecule^{-1}) for DGL adsorption onto a DLPC monolayer at the same pH and Π_i [35]. All these findings therefore reinforce the validity of our experimental approach to quantify the DGL binding onto mixed 1,2-dicaprin/Orlistat monolayers. In the present case and based on the calculated molecular area of 738 Å^2 for DGL interacting with 1,2-dicaprin monolayer, the lipase surface

occupancy (4.9% ±0.02%) was similar to the one previously determined (3.3% ±0.07%) when using DLPC films [35]. Lipase surface occupancy with a lipid film spread at the air-water interface was therefore much lower than the surface occupancy observed with the same enzyme (DGL) adsorbed onto a hydrophobic solid surface [45] (99.1% surface occupancy; 505×10^{10} molecule cm^{-2} at pH 5.0 taking into account a mean section of approximately 196×10^{-15} cm^2 for DGL molecule). As previously performed in the case of DGL interacting with a DLPC monolayer [35], it was estimated that the cross-section of DGL 3-D structure (PDB file 1K8Q in Protein Data Bank) fitting with the molecular area of 738 $Å^2$ for DGL interacting with 1,2-dicaprin monolayer at pH 5 and 25 mN m^{-1} would be located at around 12.0 Å from the protein surface when the lipase was oriented with the active site entrance facing the interface plane (Figure 6). One can thus speculate that the penetration depth of DGL in the 1,2-dicaprin monolayer is found within this range, and that the enzyme penetrates the interface in a compact form and not through a limited portion of the enzyme molecule.

By replacing the calculated value of $\Gamma_{E^*(\alpha_{Orlistat}=0)}$ in Eq. 2 and using the experimentally determined rate of 1,2-dicaprin hydrolysis by DGL in the absence of Orlistat ($v_{m\,(\alpha_{Orlistat}=0)}$ - Figure 2A, curve 1), it was possible to estimate the k_{cat}/K^*_M ratio between the interfacial catalytic rate constant (k_{cat}; s^{-1}) and the interfacial Michaëlis-Menten constant (K^*_M; molecule cm^{-2}) for DGL acting on pure 1,2-dicaprin monolayer. As shown in Figure 7, k_{cat}/K^*_M displayed a hyperbolic variation as a function of increasing DGL concentration, and reached a plateau value of around $10.7\ (\pm 0.09) \times 10^{-15}$ cm^2 $molecule^{-1}$ s^{-1} above 40 nM DGL. Such finding, also observed in τ_1 and τ_2 variations as a function of the lipase concentration in Figure 3D, suggests that 40 nM would correspond to the limiting lipase concentration beyond which no more DGL molecule is adsorbed onto the 1,2-dicaprin monolayer.

4. Conclusion

The reversibility of gastric lipase inhibition by Orlistat was shown here for the first time using the surface barostat technique and 1,2-dicaprin monolayers as substrate. This inhibition process is rather unique since Orlistat seems to form two distinct lipase-inhibitor complexes at the lipid interface. A fast covalent and reversible inhibition first allows blocking transiently the lipase activity before Orlistat is degraded and enzyme activity restored. When Orlistat mole fraction exceeds 1%, the lipase activity is however not fully restored, suggesting a secondary and irreversible binding mode for Orlistat in DGL active site. While the complete understanding of DGL inhibition by Orlistat at the interface still deserves some investigations, it seems that the presence of Orlistat mixed with 1,2-dicaprin has no significant effect on DGL adsorption/desorption equilibrium. Using mixed 1,2-dicaprin/Orlistat monolayers, it was thus possible for the first time to determine the adsorption and desorption rate constants as well as the k_{cat}/K^*_M ratio for a lipase, DGL, acting on a monomolecular film of substrate spread at the air-water interface. In conclusion, the methods and results reported here are giving access to essential kinetic parameters describing the mechanism of action of lipases on an insoluble substrate and bring new insight on the reversible inhibition of gastric lipase by Orlistat. It should be stressed however that the mechanism of DGL inhibition by Orlistat investigated here may result from specific biochemical properties of this lipase, and should not be stated as a general mode of action before additional data are obtained with other lipases.

Acknowledgements

A. Bénarouche was supported by a PhD fellowship from the Ministère de l'Enseignement Supérieur et de la Recherche. This work was supported by the CNRS and by the LISA Carnot Institute (Convention ANR n°07-CARN-009-01). Authors would like to thank Dr. R. Lebrun and R. Puppo (at the Proteomics platform of the Institut de Microbiologie de la Méditerranée, Marseille, France) for their precious help and support with the mass spectrometry experiments.

Supplementary Material

Supplementary Data (Figures S1-S2 and Table S1) associated with this article can be found in the online version.

REFERENCES

[1] F. Carrière, C. Renou, S. Ransac, V. Lopez, J. De Caro, F. Ferrato, A. De Caro, A. Fleury, P. Sanwald-Ducray, H. Lengsfeld, C. Beglinger, P. Hadvary, R. Verger, R. Laugier, Inhibition of gastrointestinal lipolysis by Orlistat during digestion of test meals in healthy volunteers, Am J Physiol Gastrointest Liver Physiol 281 (2001) G16-28.

[2] H. Lengsfeld, G. Beaumier-Gallon, H. Chahinian, A. De Caro, R. Verger, R. Laugier, F. Carrière, Physiology of Gastrointestinal Lipolysis and Therapeutical Use of Lipases and Digestive Lipase Inhibitors, in: G. Müller, and Petry, S. (Ed.), Lipases and phospholipases in drug development, Wiley-VCH, Weinheim, 2004, pp. 195-223.

[3] B. Borgstrom, Mode of action of tetrahydrolipstatin: a derivative of the naturally occurring lipase inhibitor lipstatin, Biochim. Biophys Acta 962 (1988) 308-316.

[4] P. Hadváry, H. Lengsfeld, H. Wolfer, Inhibition of pancreatic lipase in vitro by the covalent inhibitor tetrahydrolipstatin, Biochem J. 256 (1988) 357.

[5] Y. Gargouri, H. Chahinian, H. Moreau, S. Ransac, R. Verger, Inactivation of pancreatic and gastric lipases by THL and C12: 0-TNB: a kinetic study with emulsified tributyrin, Biochim. Biophys Acta 1085 (1991) 322-328.

[6] P. Hadváry, W. Sidler, W. Meister, W. Vetter, H. Wolfer, The lipase inhibitor tetrahydrolipstatin binds covalently to the putative active site serine of pancreatic lipase, J. Biol. Chem 266 (1991) 2021-2027.

[7] Q. Lüthi-Peng, H.P. Marki, P. Hadvary, Identification of the active-site serine in human pancreatic lipase by chemical modification with tetrahydrolipstatin, FEBS letters 299 (1992) 111-115.

[8] A. Tiss, H. Lengsfeld, F. Carrière, R. Verger, Inhibition of human pancreatic lipase by tetrahydrolipstatin: Further kinetic studies showing its reversibility, J Mol Cat B: Enzymatic 58 (2009) 41-47.

[9] A. Tiss, H. Lengsfeld, R. Verger, A comparative kinetic study on human pancreatic and Thermomyces lanuginosa lipases: Inhibitory effects of tetrahydrolipstatin in the presence of lipid substrates, J Mol Cat B: Enzymatic 62 (2010) 19-26.

[10] V. Belle, A. Fournel, M. Woudstra, S. Ranaldi, F. Prieri, V. Thomé, J. Currault, R. Verger, B. Guigliarelli, F. Carrière, Probing the opening of the pancreatic lipase lid using site-directed spin labeling and EPR spectroscopy, Biochemistry 46 (2007) 2205-2214.

[11] A. Tiss, S. Ransac, H. Lengsfeld, P. Hadvary, A. Cagna, R. Verger, Surface behaviour of bile salts and tetrahydrolipstatin at air/water and oil/water interfaces, Chem Phys Lipids 111 (2001) 73-85.

[12] A. Tiss, H. Lengsfeld, P. Hadvary, A. Cagna, R. Verger, Transfer of orlistat through oil-water interfaces, Chem Phys Lipids 119 (2002) 41-49.

[13] H. Stalder, G. Oesterhelt, B. Borgström, Tetrahydrolipstatin: Degradation products produced by human carboxyl-ester lipase, Helv Chim Acta 75 (1992) 1593-1603.

[14] H. Stalder, P.R. Schneider, G. Oesterhelt, Tetrahydrolipstatin: Thermal and Hydrolytic Degradation, Helv Chim Acta 73 (1990) 1022-1036.

[15] A. Aloulou, J.A. Rodriguez, S. Fernandez, D. van Oosterhout, D. Puccinelli, F. Carrière, Exploring the specific features of interfacial enzymology based on lipase studies, Biochim. Biophys Acta 1761 (2006) 995-1013.

[16] H. Singh, A. Ye, D. Horne, Structuring food emulsions in the gastrointestinal tract to modify lipid digestion, Progress in lipid research 48 (2009) 92-100.

[17] M. Golding, T.J. Wooster, The influence of emulsion structure and stability on lipid digestion, Current Opinion in Colloid & Interface Science 15 (2010) 90-101.

[18] J.F. Cavalier, S. Ransac, R. Verger, G. Buono, Inhibition of human gastric and pancreatic lipases by chiral alkylphosphonates. A kinetic study with 1,2-didecanoyl-sn-glycerol monolayer, Chem Phys Lipids 100 (1999) 3-31.

[19] V. Delorme, R. Dhouib, S. Canaan, F. Fotiadu, F. Carrière, J.-F. Cavalier, Effects of Surfactants on Lipase Structure, Activity and Inhibition, Pharm. Res 28 (2011) 1831-1842.

[20] H. Haiker, H. Lengsfeld, P. Hadvary, F. Carrière, Rapid exchange of pancreatic lipase between triacylglycerol droplets, Biochimica et Biophysica Acta (BBA)-Lipids and Lipid Metabolism 1682 (2004) 72-79.

[21] G. Pieroni, R. Verger, Hydrolysis of mixed monomolecular films of triglyceride/lecithin by pancreatic lipase, J. Biol. Chem 254 (1979) 10090-10094.

[22] Y. Gargouri, G. Piéroni, C. Rivière, L. Sarda, R. Verger, Inhibition of lipases by proteins: A binding study using dicaprin monolayers, Biochemistry 25 (1986) 1733-1738.

[23] M. Aoubala, M. Ivanova, I. Douchet, A. De Caro, R. Verger, Interfacial binding of human gastric lipase to lipid monolayers, measured with an ELISA, Biochemistry 34 (1995) 10786-10793.

[24] F. Marguet, I. Douchet, J.F. Cavalier, G. Buono, R. Verger, Interfacial and or molecular recognition by lipases of mixed monomolecular films of 1,2-dicaprin and chiral organophosphorus glyceride analogues?, Colloids Surf B: Biointerfaces 13 (1999) 37-45.

[25] A. Tiss, F. Carrière, I. Douchet, S. Patkar, A. Svendsen, R. Verger, Interfacial binding and activity of lipases at the lipid–water interface: effects of Gum Arabic and surface pressure, Colloids Surf. B: Biointerfaces 26 (2002) 135-145.

[26] J.-C. Bakala N'Goma, S. Amara, K. Dridi, V. Jannin, F. Carrière, Understanding the lipid-digestion processes in the GI tract before designing lipid-based drug-delivery systems, Therapeutic Delivery 3 (2011) 105-124.

[27] A. Roussel, N. Miled, L. Berti-Dupuis, M. Rivière, S. Spinelli, P. Berna, V. Gruber, R. Verger, C. Cambillau, Crystal structure of the open form of dog gastric lipase in complex with a phosphonate inhibitor, J. Biol. Chem 277 (2002) 2266-2274.

[28] S. Fernandez, S. Chevrier, N. Ritter, B. Mahler, F. Demarne, F. Carrière, V. Jannin, In vitro gastrointestinal lipolysis of four formulations of piroxicam and cinnarizine with the self

emulsifying excipients Labrasol and Gelucire 44/14, Pharmaceutical Research 26 (2009) 1901-1910.

[29] V. Gruber, P. Berna, T. Arnaud, P. Bournat, C. Clément, D. Mison, B. Olagnier, L. Philippe, M. Theisen, S. Baudino, C. Bénicourt, C. Cudrey, C. Bloës, N. Duchateau, S. Dufour, C. Gueguen, S. Jacquet, C. Ollivo, C. Poncetta, N. Zorn, D. Ludevid, A. Van Dorsselaer, R. Verger, A. Doherty, B. Mérot, C. Danzin, Large-scale production of a therapeutic protein in transgenic tobacco plants: effect of subcellular targeting on quality of a recombinant dog gastric lipase, Molecular Breeding 7 (2001) 329-340.

[30] V. Point, K.V.P. Pavan Kumar, S. Marc, V. Delorme, G. Parsiegla, S. Amara, F. Carrière, G. Buono, F. Fotiadu, S. Canaan, J. Leclaire, J.-F. Cavalier, Analysis of the discriminative inhibition of mammalian digestive lipases by 3-phenyl substituted 1,3,4-oxadiazol-2(3*H*)-ones, European Journal of Medicinal Chemistry 58 (2012) 452-463.

[31] R. Verger, M.C. Mieras, G.H. de Haas, Action of phospholipase A at interfaces, J. Biol. Chem 248 (1973) 4023-4034.

[32] L. Wilhelmy, Ueber die Abhängigkeit der Capillaritäts Constanten des Alkohols von Substanz und Gestalt des benetzten festen Körpers, Annalen der Physik 195 (1863) 177-217.

[33] I. Panaiotov, R. Verger, Enzymatic reactions at interfaces: Interfacial and temporal organization of enzymatic lipolysis, in: W. Norde (Ed.), Physical Chemistry of Biological Interfaces, Marcel Dekker, Inc, New York, Basel, 2000, pp. 359-400.

[34] R. Verger, G.H. De Haas, Enzyme reactions in a membrane model. 1. A new technique to study enzyme reactions in monolayers, Chem Phys Lipids 10 (1973) 127-136.

[35] A. Bénarouche, V. Point, G. Parsiegla, F. Carrière, J.-F. Cavalier, New insights into the pH-dependent interfacial adsorption of dog gastric lipase using the monolayer technique, Colloids Surf. B: Biointerfaces 111 (2013) 306-312.

[36] R. Verger, G.H. De Haas, Interfacial enzyme kinetics of lipolysis, Annual review of biophysics and bioengineering 5 (1976) 77-117.

[37] R. Verger, J. Rietsch, M. Van Dam-Mieras, G. De Haas, Comparative studies of lipase and phospholipase A2 acting on substrate monolayers, J. Biol. Chem 251 (1976) 3128-3133.

[38] D.J.C. Pappin, P. Hojrup, A.J. Bleasby, Rapid identification of proteins by peptide-mass fingerprinting, Curr. Biol. 3 (1993) 327-332.

[39] S. Ransac, Y. Gargouri, H. Moreau, R. Verger, Inactivation of pancreatic and gastric lipases by tetrahydrolipstatin and alkyl-dithio-5-(2-nitrobenzoic acid). A kinetic study with 1,2-didecanoyl-sn-glycerol monolayers, Eur. J Biochem 202 (1991) 395-400.

[40] Y. Gargouri, S. Ransac, R. Verger, Covalent inhibition of digestive lipases: an in vitro study, Biochim. Biophys Acta 1344 (1997) 6-37.

[41] G. Piéroni, R. Verger, Hydrolysis of mixed monomolecular films of phosphatidylcholine/triacylglycerol by pancreatic phospholipase A_2, Eur. J. Biochem. 132 (1983) 639-644.

[42] P. Vainio, J.A. Virtanen, P.K.J. Kinnunen, J. Gotto, Antonio M., J.T. Sparrow, F. Pattus, P. Bougis, R. Verger, Action of lipoprotein lipase on mixed triacylglycerol/phosphatidylcholine monolayers. Activation by apolipoprotein C-II, J. Biol. Chem. 258 (1983) 5477-5482.

[43] I. Arimoto, M. Fujita, H. Saito, T. Handa, K. Miyajima, Activation and inhibition of lipoprotein lipase in mixed monolayers of medium or long chain-triglycerides and phospholipids, Colloid & Polymer Science 275 (1997) 60-66.

[44] G.H. Peters, U. Dahmen-Levison, K. de Meijere, G. Brezesinski, S. Toxvaerd, H. Möhwald, A. Svendsen, P.K.J. Kinnunen, Influence of Surface Properties of Mixed Monolayers on Lipolytic Hydrolysis, Langmuir 16 (2000) 2779-2788.

[45] H. Chahinian, T. Snabe, C. Attias, P. Fojan, S.B. Petersen, F. Carrière, How gastric lipase, an interfacial enzyme with a Ser-His-Asp catalytic triad, acts optimally at acidic pH, Biochemistry 45 (2006) 993-1001.

[46] P. Bougis, H. Rochat, G. Pieroni, R. Verger, Penetration of phospholipid monolayers by cardiotoxins, Biochemistry 20 (1981) 4915-4920.

Figure Captions

Scheme 1. *Structure of Orlistat (**A**), its mode of action in lipase inhibition (**B**) and its degradation products (**C**).* Panel B shows a schematic representation of the nucleophilic attack of the *β*-lactone ring of Orlistat by the lipase active site serine residue leading to the formation of the long-lived acyl-enzyme complex **1**. Hydrolysis of this covalent adduct releases the active enzyme and provides the *β*-hydroxy carboxylic acid **2** as the primary product. Compound **2** is then isomerised either to **3** by migration of the *N*-formyl-L-leucine group (NFL) of Orlistat or loses NFL by hydrolysis to give dihydroxy acid **4**. Ring closure of **4** furnishes 4-hydroxy-*δ*-lactone **6**, a compound also accessible *via* **3** which, after cyclization to *δ*-lactone **5** and subsequent hydrolysis provides **6**. Adapted from references [3, 13, 14].

Figure 1. **(A)** *Surface pressure versus molecular area (Π–A) curves of mixed 1,2-dicaprin/Orlistat monomolecular films* and **(B-C)** *variation in the mean molecular area as a function of the Orlistat mole fraction in mixed films at a selected surface pressure of 25 mN* m^{-1}. The mixed monolayer was formed over the surface of a rectangular Teflon trough (volume 126.3 mL; surface area, 210.5 cm^2) filled with 10 mM sodium acetate buffer (pH 5.0) containing 100 mM NaCl and 20 mM $CaCl_2$. The prepared monolayer was left for at least 10 min at 25 °C until stabilization. **(A)** The Π–*A* isotherms were recorded by monitoring the surface pressure increase during film compression with the mobile barrier at a constant rate of 6.1 $cm^2\ min^{-1}$. Based on the trough dimensions and the amounts of lipids spread at the air-water interface, the barrier movement corresponded to a film compression of 3.0 $Å^2\ molecule^{-1}\ min^{-1}$. These compression isotherms are representative of individual experiments performed in triplicate (CV% < 5%). **(B)** Mean molecular areas measured for various mixed films ranging from pure 1,2-dicaprin to pure Orlistat. **(C)** Blow-up view showing the variations in the mean molecular areas for Orlistat mole fractions ($\alpha_{Orlistat}$) ranging from 0 to 1.5%. Data obtained from the

compression isotherms depicted in **panel A** are presented as mean values ± standard deviations (n=3; CV% < 5.0%).

Figure 2. *Monomolecular film experiments using the surface barostat mode at 25 mN m^{-1} and pH 5*. **(A)** Typical kinetic recordings of the mobile barrier shift *vs*. time upon the hydrolysis by DGL of 1,2-dicaprin monolayers containing variable amounts of Orlistat. The dashed line corresponds to the asymptote reached under steady-state conditions, and τ_1 (lag time) is the intercept with time axis of this asymptote. The $\Delta L_{barrier}$ value (mm) represents the backward movement from the initial zero-position of the mobile barrier observed during lag-times. **(B-C)** Variation of DGL residual activity ($RA_{E^*(\%)}$, % - Eq. 3) measured under the steady state conditions as a function of Orlistat mole fraction in the mixed film. **(D)** Variation of the mobile barrier movement *vs*. time in presence (60 nM final concentration) or absence of DGL injected under a pure Orlistat monolayer spread over both compartments. All assays were carried out at 25 °C in a "zero order" trough at a constant Π_i of 25 mN m^{-1} as described in **Material and Methods** section. DGL final concentration ranged from 8.4 nM (panels **A** and **B**) to 60 nM (panels **C** and **D**). All data are presented as mean values ± standard deviations (n=3; CV% < 5%).

Figure 3. *Determination of τ_1 and τ_2 characteristic times*. (**A**) Typical variation in surface pressure recorded after injection of DGL below a mixed monomolecular film of 1,2-dicaprin/Orlistat (99.5:0.5, mol/mol) spread at 25 mN m^{-1} over a buffer at pH 5.0. **(B)** typical hydrolysis kinetics of the same mixed monolayer spread at 25 mN m^{-1} monitored with the surface barostat mode, The "induction" time τ_2 showed in panel **A** was estimated from the inflexion point on the $\Delta\Pi = f(t)$ curve where the surface pressure suddenly decreased after reaching a maximum value. Lag time τ_1 in panel **B** was calculated from the intercept with time

axis of the asymptote reached under steady state conditions (dashed-line). **(C)** Variations of both τ_1 and τ_2 as a function of Orlistat mole fraction ($\alpha_{Orlistat} \leq 1.5\%$) in the mixed film. **(D)** Variations of both τ_1 and τ_2 as a function of the DGL concentration in the subphase at $\alpha_{Orlistat}$ = 0.5%. Assays were carried out at a working surface pressure of 25 mN m^{-1} for both adsorption kinetics and enzyme kinetics as described in **Material and Methods** section. DGL final concentration ranged from 8.4 nM (panels **A**, **B** and **C**) to 60 nM (panel **D**). All data are presented as mean values ± standard deviations (n=3; CV% < 5%).

Figure 4. *Proposed kinetic model illustrating the inhibition/reactivation of DGL in presence of Orlistat at the lipid interface*. Symbols and abbreviations are as follows : E, free enzyme concentration in the bulk phase (molecule/volume); *E**, interfacial enzyme concentration (molecule/surface); *S**, interfacial concentration of substrate (molecule/surface); *E***S*, interfacial enzyme-substrate complex concentration (molecule/surface); I^*_c, interfacial concentration of the reactive Orlistat molecule with the closed β-lactone ring (molecule/surface); E^*I_o, interfacial concentration of the covalent enzyme-Orlistat complex with the open β-lactone ring (molecule/surface); I^*_h, interfacial concentration of Orlistat degradation product resulting from the hydrolysis of β-lactone (molecule/surface); I_d, bulk concentration of soluble Orlistat degradation products generated after β-lactone ring opening, after their desorption from the lipid interface (molecule/volume); E^*I_2, interfacial concentration of the enzyme complexed with Orlistat in a secondary and irreversible binding mode; P, soluble lipolysis product concentration resulting from 1,2-dicaprin lipolysis (molecule/volume); k_d, desorption rate constant ($time^{-1}$); k_a, adsorption rate constant ($volume.molecule^{-1}.time^{-1}$); k_{cat}, catalytic rate constant ($time^{-1}$); K^*_M, interfacial Michaelis-Menten constant (molecule/surface).

Figure 5. Variation of **(A)** the adsorption equilibrium coefficient (K_{Ads}) and **(B)** the surface concentration of adsorbed DGL (Γ_{E*}) as a function of the Orlistat mole fraction ($\alpha_{Orlistat} \leq 1.0\%$) in the mixed 1,2-dicaprin/Orlistat film spread at a surface pressure of 25 mN m^{-1} over a buffer at pH 5.0. **(C)** Variations of the apparent molecular areas (A_{E*}) of the adsorbed DGL as a function of the relative surface increase ($\Delta S/S$) of mixed 1,2-dicaprin/Orlistat films spread at 25 mN m^{-1}. K_{Ads} was derived from the ratio of the measured rate constants ($K_{Ads} = k_a/k_d$) determined from curve fitting adsorption curves with Eq. 4. Γ_{E*} and A_{E*} were estimated by indirect calculation using Eqs 5 and 6, respectively. Data are presented as mean values ± standard deviations (n=3; CV% < 5.0%).

Figure 6. *Putative orientation of DGL penetrating into a 1,2-dicaprin monolayer spread at 25 mN m^{-1}*. The structure of the DGL is shown as ribbon (panel A) and molecular surface (panels B-C) representations. Hydrophobic residues (Ala, Leu, Ile, Val, Trp, Tyr, Phe, Pro, Met) are highlighted in white, and the catalytic Ser153 is coloured in red. **(A)** Side view of the DGL molecule oriented at the lipid interface. **(B)** Top view of the DGL showing the hydrophobic ring surrounding the active site entrance and parallel to the putative lipid interface. **(C)** Top view of DGL cross-section (purple colour) made parallel to the interface plane. The position of the cross-section, corresponding to the estimated molecular area $A_{E*(\alpha_{Orlistat}=0)} = 738 \pm 22$ $Å^2$ $molecule^{-1}$, and its distance from the top of the DGL molecule is indicated in panel **A**. These models were drawn using PyMOL Molecular Graphics System (Version 1.3, Schrödinger, LLC) and the 1K8Q Protein Data Bank file for DGL 3-D structure with the lid in the open conformation.

Figure 7. Variation of the interfacial specificity constant (k_{cat}/K^*_M) of DGL acting on pure 1,2-dicaprin monolayers, as a function of the lipase concentration in the subphase. k_{cat}/K^*_M

values were estimated by indirect calculation using Eq. 2. Data are presented as mean values ± standard deviations (n=3; CV% < 5.0%).

Table 1. Values of τ_1 lag time and ΔS surface increase determined for various lipase concentration (C_{E0} = 8.4 to 60 nM) during DGL kinetics with 1,2-dicaprin monolayer containing variable mole fractions ($\alpha_{Orlistat}$) of Orlistat at Π_i = 25 mN m^{-1}.[a]

$\alpha_{Orlistat}$	τ_1 (min)				ΔS (cm^2)				Mean $\Delta S/S$
	8.4 nM	20 nM	40 nM	60 nM	8.4 nM	20 nM	40 nM	60 nM	
0.3%	18.3 ±0.7	8.8 ±0.4	5.7 ±0.1	4.3 ±0.2	1.34	1.28	1.30	1.32	4.2%
0.5%	26.0 ±0.6	12.0 ±0.4	7.5 ±0.3	7.2 ±0.1	2.35	2.28	2.12	2.38	7.3%
1.0%	53.5 ±1.7	15.7 ±0.7	9.9 ±0.2	6.1 ±0.3	3.34	3.54	3.30	3.26	10.8%
1.5%	74.6 ±2.5	ND	ND	ND	5.37	ND	ND	ND	17.2%

[a] ND: not determined. Mean $\Delta S/S$ (S = 31.2 cm^2) represents the relative surface increase in the reaction compartment of the "zero-order" Teflon trough. Data are presented as mean values ± standard deviations of three independent assays (CV% < 5.0%).

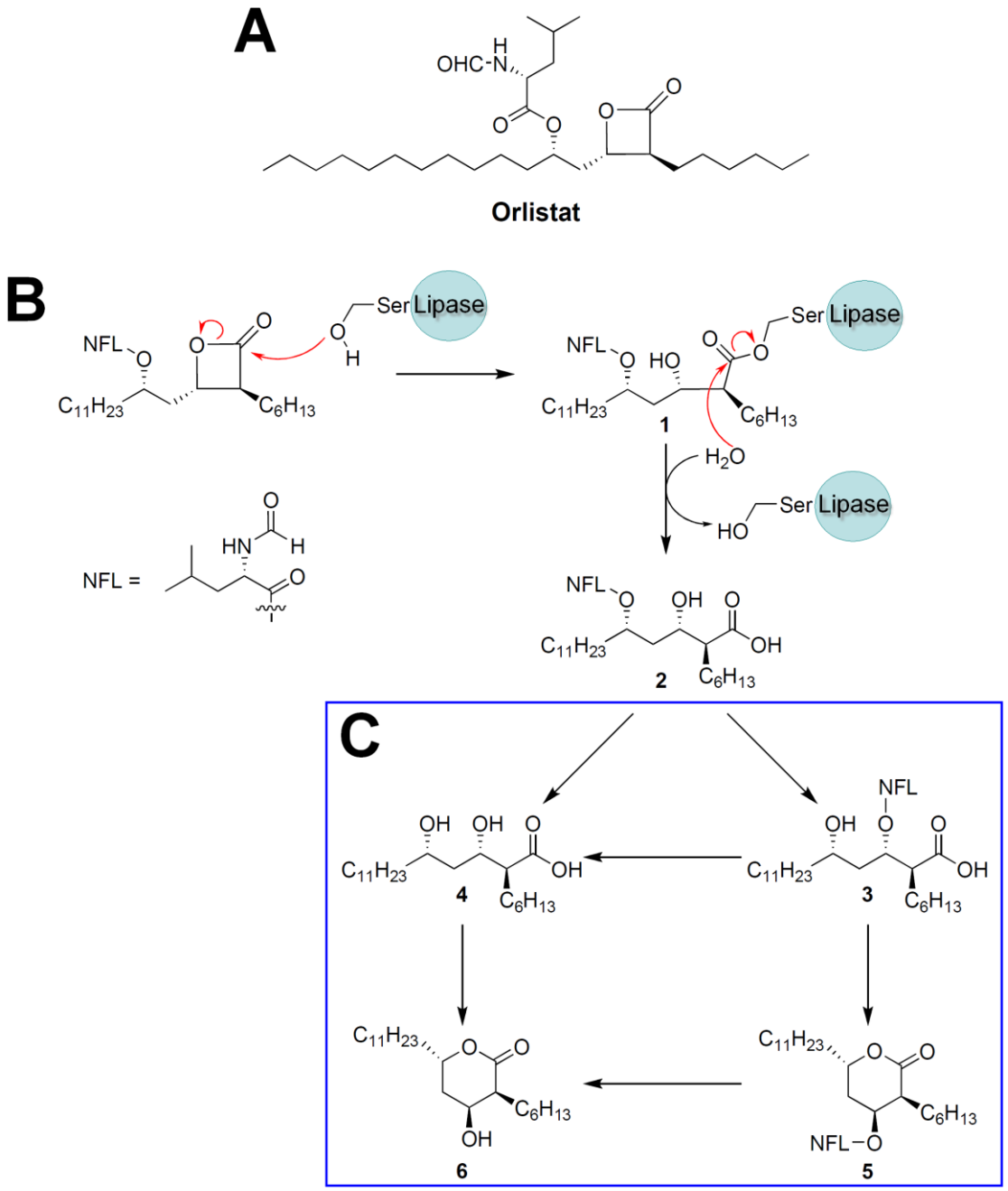
A
OHC-N
H
O
O
O
O
Orlistat
B
NFL
O
O
O
H
Ser
Lipase
C11H23
C6H13
NFL =
HN
H
O
O
NFL
O
HO
O
O
Ser
Lipase
C11H23
C6H13
1
H2O
HO
Ser
Lipase
NFL
O
OH
O
OH
C11H23
C6H13
2
C
OH
OH
O
OH
C11H23
C6H13
4
NFL
OH
O
O
OH
C11H23
C6H13
3
C11H23
O
O
C6H13
OH
6
C11H23
O
O
C6H13
NFL
O
5

Scheme 1

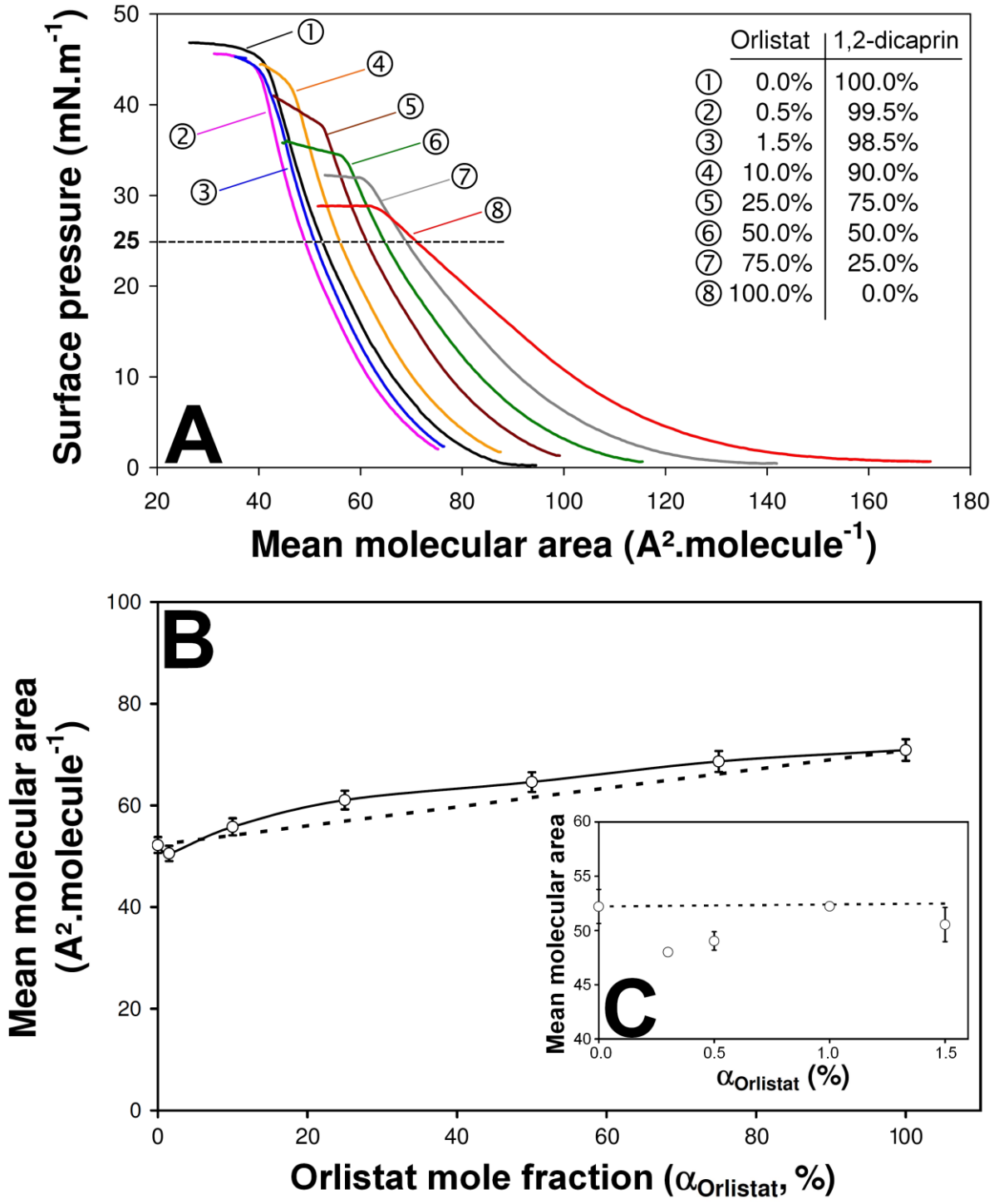
Surface pressure (mN.m-1)
Mean molecular area (A².molecule-1)
A
Orlistat | 1,2-dicaprin
① 0.0% 100.0%
② 0.5% 99.5%
③ 1.5% 98.5%
④ 10.0% 90.0%
⑤ 25.0% 75.0%
⑥ 50.0% 50.0%
⑦ 75.0% 25.0%
⑧ 100.0% 0.0%
B
Mean molecular area (A².molecule-1)
Orlistat mole fraction (αOrlistat, %)
C
Mean molecular area
αOrlistat (%)

Figure 1

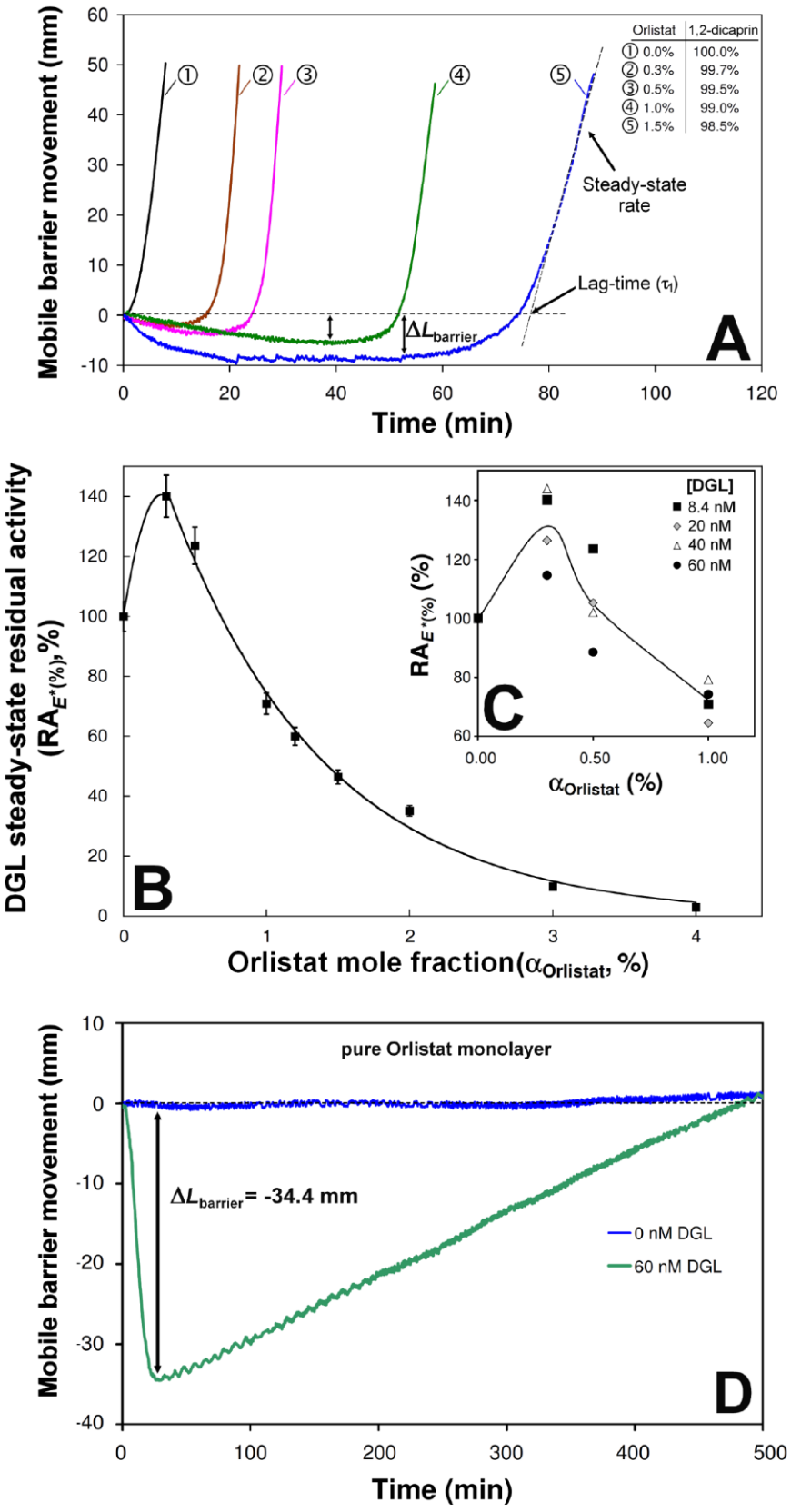
Mobile barrier movement (mm)
Time (min)
Orlistat
1,2-dicaprin
① 0.0% 100.0%
② 0.3% 99.7%
③ 0.5% 99.5%
④ 1.0% 99.0%
⑤ 1.5% 98.5%
Steady-state rate
Lag-time (τl)
ΔLbarrier
A
DGL steady-state residual activity (RAE*(%), %)
Orlistat mole fraction(αOrlistat, %)
[DGL]
8.4 nM
20 nM
40 nM
60 nM
RAE*(%) (%)
αOrlistat (%)
C
B
pure Orlistat monolayer
ΔLbarrier= -34.4 mm
0 nM DGL
60 nM DGL
D

Figure 2

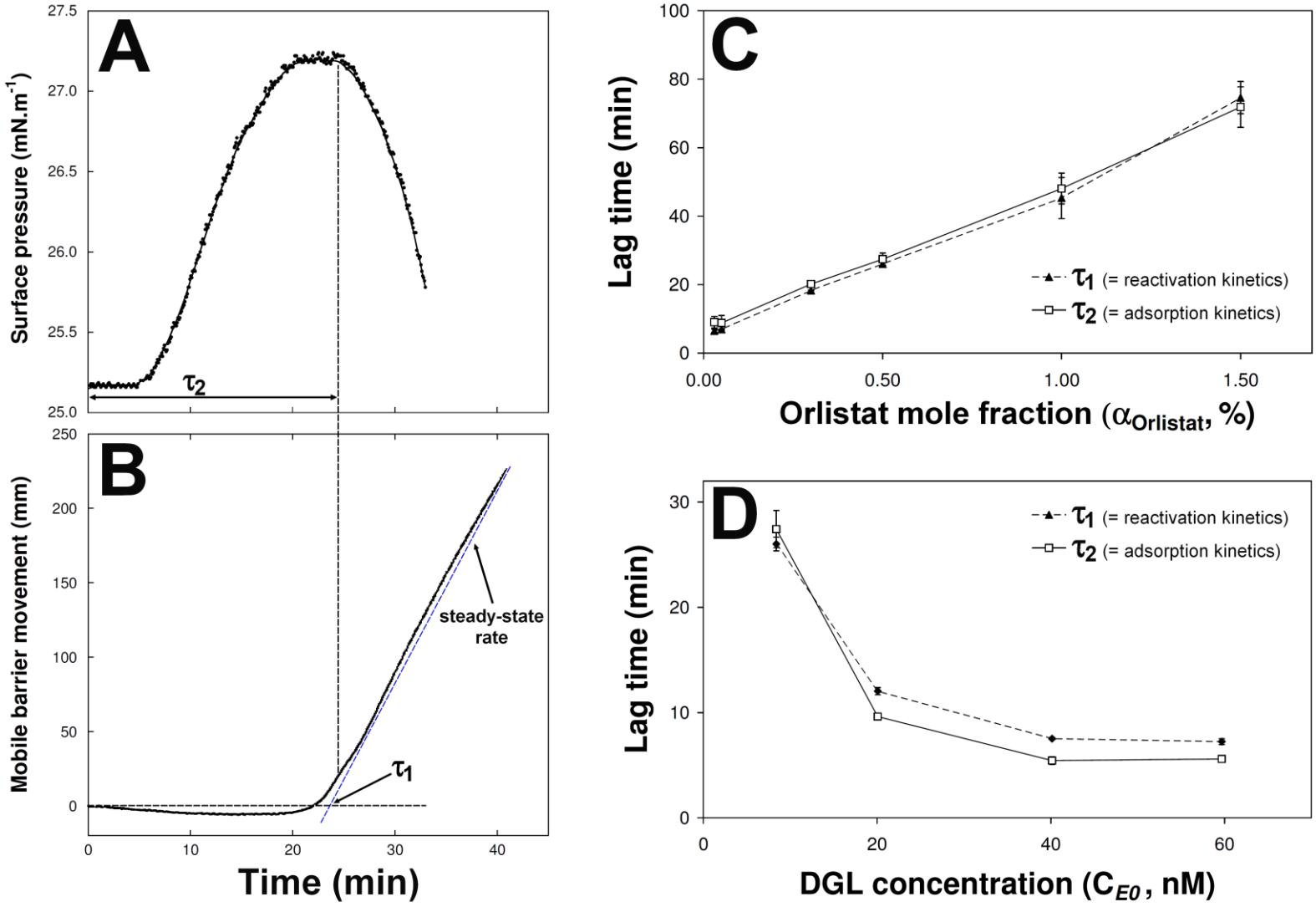
A
Surface pressure (mN.m-1)
27.5
27.0
26.5
26.0
25.5
25.0
τ2
B
Mobile barrier movement (mm)
250
200
150
100
50
0
steady-state rate
τ1
0
10
20
30
40
Time (min)
C
Lag time (min)
100
80
60
40
20
0
τ1 (= reactivation kinetics)
τ2 (= adsorption kinetics)
0.00
0.50
1.00
1.50
Orlistat mole fraction (αOrlistat, %)
D
Lag time (min)
30
20
10
0
τ1 (= reactivation kinetics)
τ2 (= adsorption kinetics)
0
20
40
60
DGL concentration (CE0, nM)

Figure 3

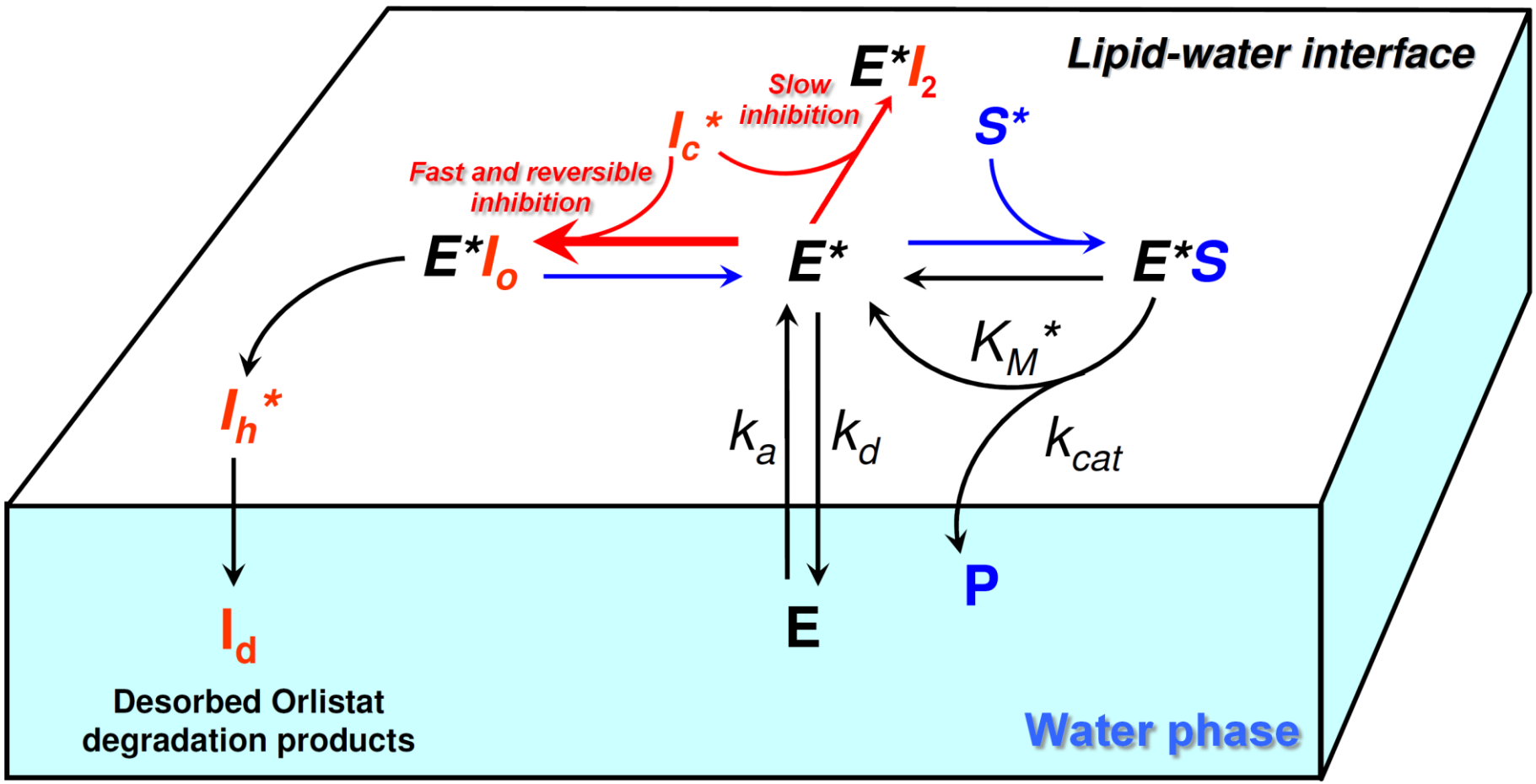
Lipid-water interface
E*I2
Slow inhibition
Ic*
Fast and reversible inhibition
S*
E*Io
E*
E*S
KM*
Ih*
ka
kd
kcat
P
E
Id
Desorbed Orlistat degradation products
Water phase

Figure 4

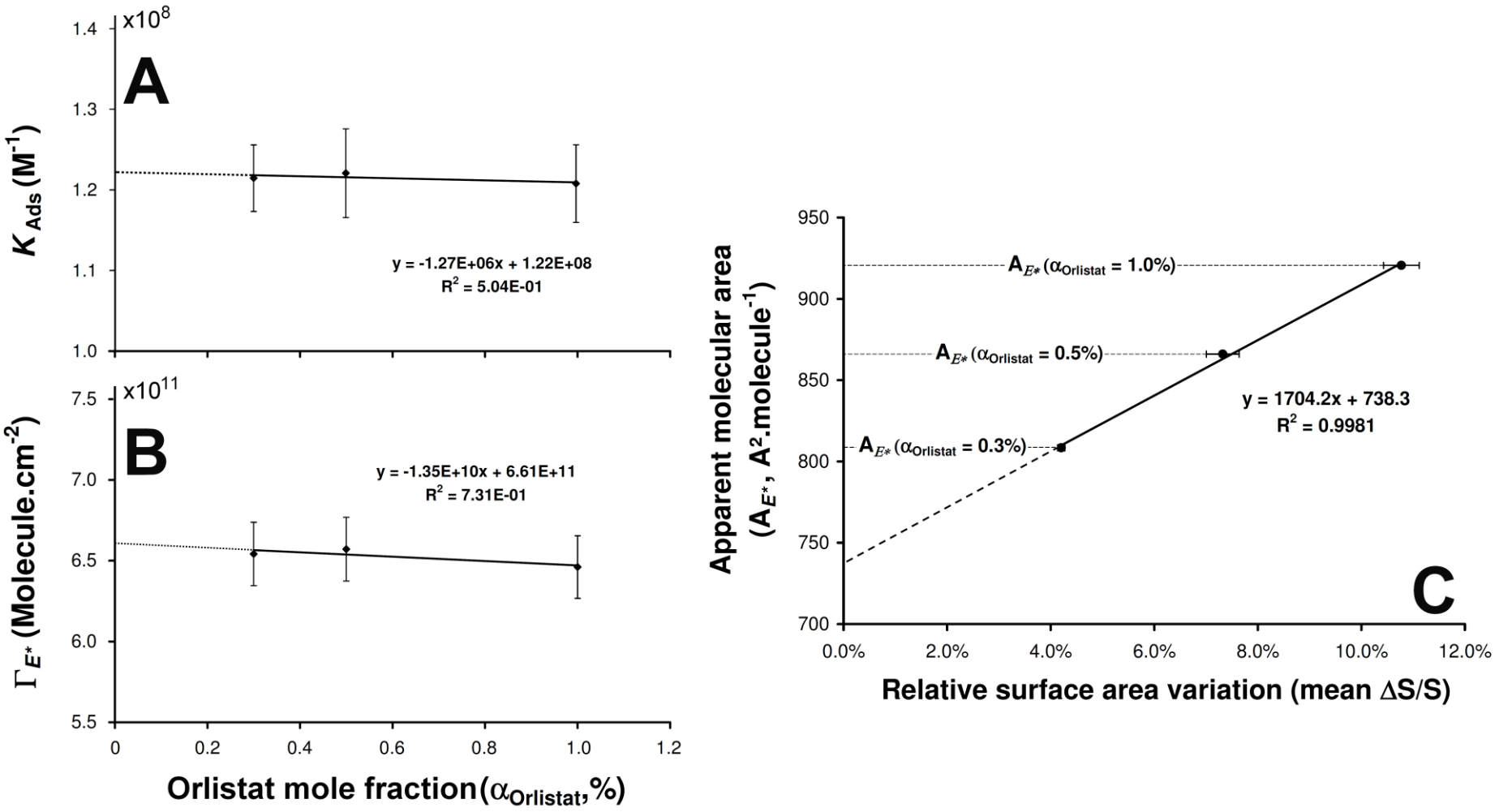
A
x10^8
K Ads (M^-1)
y = -1.27E+06x + 1.22E+08
R^2 = 5.04E-01
B
x10^11
Γ E* (Molecule.cm^-2)
y = -1.35E+10x + 6.61E+11
R^2 = 7.31E-01
Orlistat mole fraction(αOrlistat,%)
C
Apparent molecular area (AE*, A².molecule^-1)
AE* (αOrlistat = 1.0%)
AE* (αOrlistat = 0.5%)
AE* (αOrlistat = 0.3%)
y = 1704.2x + 738.3
R^2 = 0.9981
Relative surface area variation (mean ΔS/S)

Figure 5

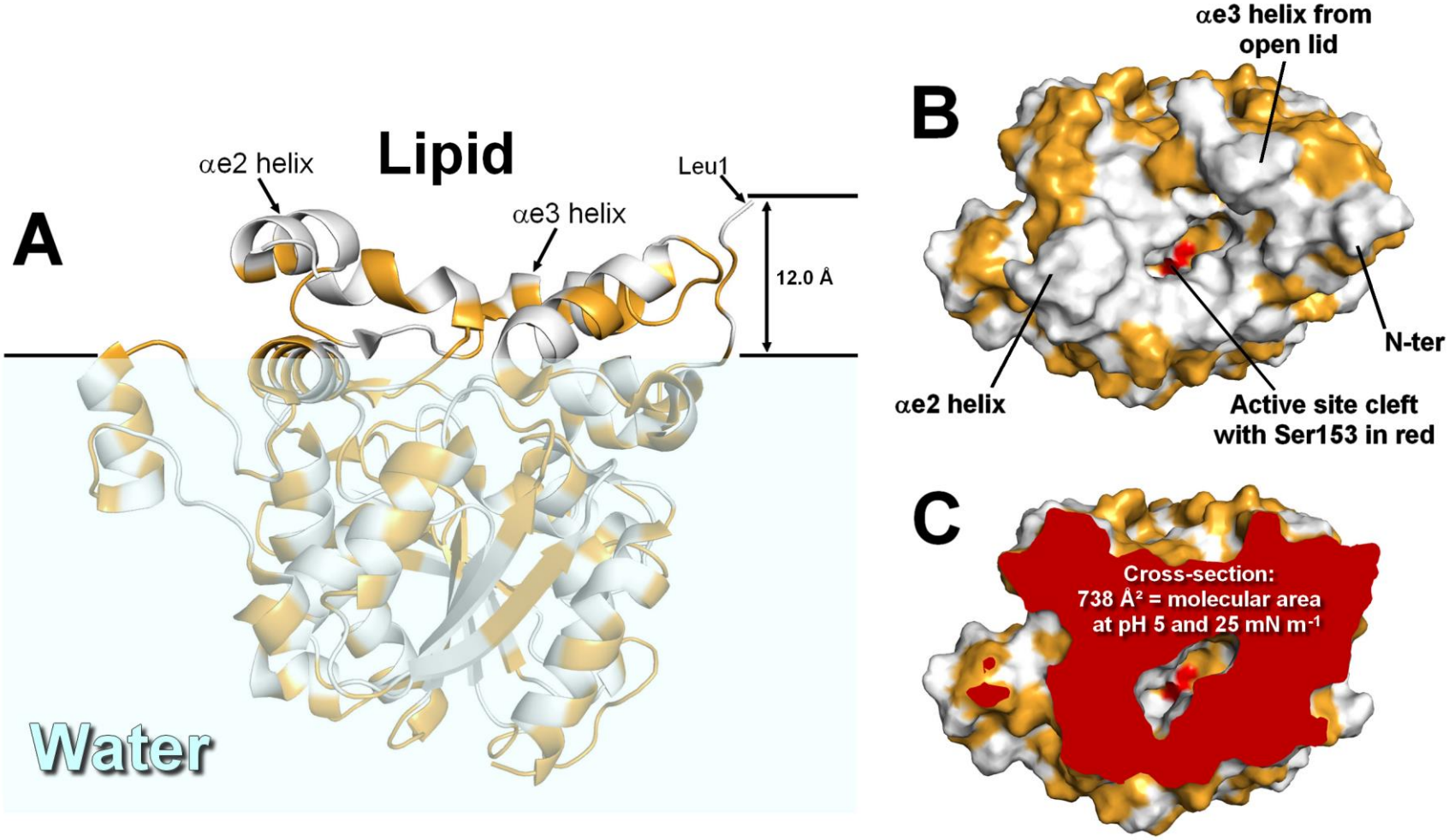
A
Lipid
αe2 helix
αe3 helix
Leu1
12.0 Å
Water
B
αe3 helix from
open lid
αe2 helix
Active site cleft
with Ser153 in red
N-ter
C
Cross-section:
738 Å² = molecular area
at pH 5 and 25 mN m⁻¹

Figure 6

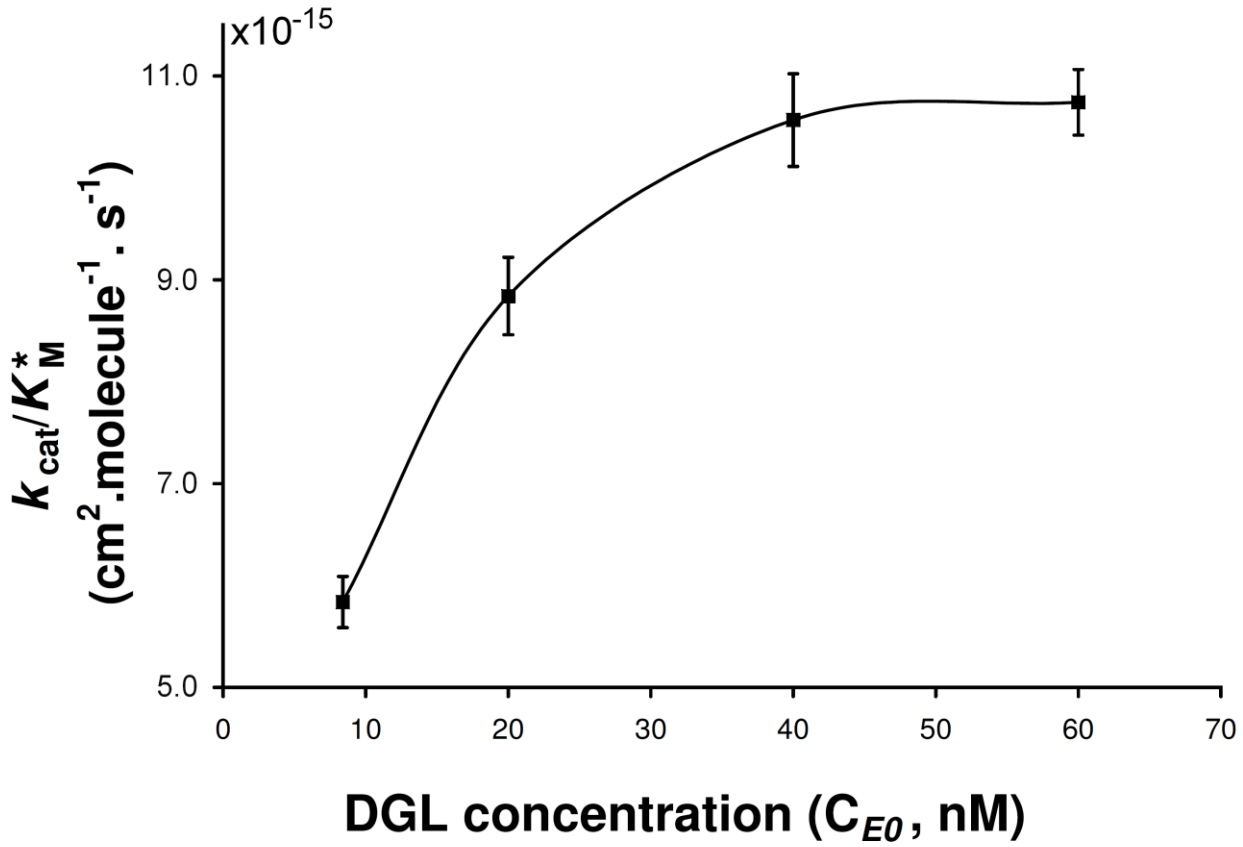
x10-15
11.0
9.0
7.0
5.0
0
10
20
30
40
50
60
70
kcat/K*M
(cm2.molecule-1. s-1)
DGL concentration (CE0, nM)

Figure 7